British Journal of Pharmacology

British Journal of Pharmacology (2017) **174** 4493–4507 4493

RESEARCH PAPER

Human podocytes express functional thermosensitive TRPV channels

Correspondence Tamás Bíró, Department of Immunology, Faculty of General Medicine, University of Debrecen, H-4032 Debrecen, Egyetem tér 1, Hungary. E-mail: biro.tamas@med.unideb.hu

Received 25 October 2016; **Revised** 16 August 2017; **Accepted** 10 September 2017

Lídia Ambrus[1], Balázs Kelemen[1], Tamás Szabó[2], Tamás Bíró[1,3,*] and Balázs István Tóth[1,*]

[1]DE-MTA 'Lendület' Cellular Physiology Research Group, Department of Physiology, Medical Faculty, University of Debrecen, Debrecen, Hungary, [2]Department of Pediatrics, Medical Faculty, University of Debrecen, Debrecen, Hungary, and [3]Department of Immunology, Medical Faculty, University of Debrecen, Debrecen, Hungary

*T.B. and B.I.T. contributed equally to the work.

BACKGROUND AND PURPOSE

Heat-sensitive transient receptor potential vanilloid (TRPV) channels are expressed in various epithelial tissues regulating, among else, barrier functions. Their expression is well established in the distal nephron; however, we have no data about their presence in podocytes. As podocytes are indispensable in the formation of the glomerular filtration barrier, we investigated the presence and function of Ca^{2+}-permeable TRPV1–4 channels in human podocyte cultures.

EXPERIMENTAL APPROACH

Expression of TRPV1–4 channels was investigated at protein (immunocytochemistry, Western blot) and mRNA (Q-PCR) level in a conditionally immortalized human podocyte cell line. Channel function was assessed by measuring intracellular Ca^{2+} concentration using Flou-4 Ca^{2+}-indicator dye and patch clamp electrophysiology upon applying various activators and inhibitors.

KEY RESULTS

Thermosensitive TRP channels were expressed in podocytes. The TRPV1-specific agonists capsaicin and resiniferatoxin did not affect the intracellular Ca^{2+} concentration. Cannabidiol, an activator of TRPV2 and TRPV4 channels, induced moderate Ca^{2+}-influxes, inhibited by both tranilast and HC067047, blockers of TRPV2 and TRPV4 channels respectively. The TRPV4-specific agonists GSK1016790A and 4α-phorbol 12,13-didecanoate induced robust Ca^{2+}-signals which were abolished by HC067047. Non-specific agonists of TRPV3 channels induced marked Ca^{2+} transients. However, TRPV3 channel blockers, ruthenium red and isopentenyl diphosphate only partly inhibited the responses and TRPV3 silencing was ineffective suggesting remarkable off-target effects of the compounds.

CONCLUSION AND IMPLICATIONS

Our results indicate the functional presence of TRPV4 and other thermosensitive TRPV channels in human podocytes and raise the possibility of their involvement in the regulation of glomerular filtration barrier.

Abbreviations

2-APB, 2-aminoethoxydiphenyl borate; 4α-PDD, 4α-phorbol 12,13-didecanoate; CBD, cannabidiol; FSGS, focal segmental glomerulosclerosis; IP_3, inositol trisphosphate; IPP, isopentenyl diphosphate; PPIA, peptidylprolyl isomerase A; Q-PCR, quantitative real-time PCR

DOI:10.1111/bph.14052

Introduction

Among **voltage gated ion channels**, the **transient receptor potential (TRP) ion channels** form a heterogeneous group with diverse functions. They are sensitive to various physical stimuli, like osmotic challenges, mechanical stimulation, changes of membrane potential or environmental temperature. Therefore, they are generally considered as multimodal cellular sensors. Moreover, TRP channels possess marked chemosensitivity, as well. They can be activated or inhibited by several endogenous or exogenous chemical ligands opening a huge field for potential pharmacological interventions (Nilius and Szallasi, 2014). Among TRP channels, the thermosensitive members are the most pursued drug targets especially because of their vital role in several sensory functions (Moran *et al.,* 2011). However, thermoTRPs, especially the heat-sensitive members of the TRP vanilloid (TRPV) subfamily, play an emerging role in epithelial biology and barrier functions, as well (Moran *et al.,* 2011; Nilius and Szallasi, 2014). They are widely expressed in the outer and inner linings of the human body, in the skin (Tóth *et al.,* 2014), airway epithelia (Grace *et al.,* 2014), endothelium (Earley and Brayden, 2015) or reabsorbing epithelium of kidney tubules (Kassmann *et al.,* 2013).

Several TRP channels are expressed along the nephron playing important (patho)physiological roles in kidney functions (Woudenberg-Vrenken *et al.,* 2009). **TRPV5**, **TRPV6** and **TRPM6** channels, expressed in the apical membrane of distal tubule epithelium, play an essential role in ion homeostasis *via* ensuring physiological reabsorption of Ca^{2+} and Mg^{2+} respectively (Dimke *et al.,* 2011). Mutations in the **TRPP 1/2** complex serve as etiological factors in the development of polycystic kidney disease (Retailleau and Duprat, 2014; Tóth and Nilius, 2015). The **TRPC6** channel regulates podocyte function influencing the integrity of the glomerular filtration barrier and playing an etiological role in different proteinuric diseases, including familial focal segmental glomerulosclerosis (FSGS) (Dryer and Reiser, 2010; Tóth and Nilius, 2015).

Regarding the heat-sensitive TRPV channels, **TRPV4** is expressed in various segments of the urogenital tract, involving distal tubules of the kidney, and it plays an important role in cell junction and barrier formation (Janssen *et al.,* 2016). The presence of **TRPV1** channels was also shown in the tubules of the renal cortex and medulla as well as in the wall of the renal pelvis (Feng *et al.,* 2008; Kassmann *et al.,* 2013). Moreover, both TRPV1 and TRPV4 channels can influence endothelial barrier functions (Alvarez *et al.,* 2006; Yang *et al.,* 2010) which can affect the vascular side of the glomerular filtration barrier. However, we do not have any data about the expression of these channels in the other component of the glomerular filtration barrier, that is, the podocytes of Bowman's capsule. Therefore, in the current study, we aimed at investigating the molecular expression and functionality of heat-sensitive TRPV1–4 channels in human podocytes using a conditionally immortalized human podocyte cell culture system.

Methods

Cell cultures

The human podocyte cell line provided by Prof. Hermann Pavenstädt (University Hospital of Münster, Münster, Germany) was established and cultured as described previously (Saleem *et al.,* 2002; Ambrus *et al.,* 2015). In brief, cells were cultured in 'permissive' condition in RPMI medium (PAA Laboratories GmbH, Pasching, Austria) supplemented with 10% fetal bovine serum (Invitrogen, Paisley, UK), 50 $U{\cdot}mL^{-1}$ penicillin, 50 $\mu g{\cdot}mL^{-1}$ streptomycin, 1.25 $\mu g{\cdot}mL^{-1}$ Fungizone (both from PPA Laboratories GmbH) and insulin-transferrin-selenium (1:100; Invitrogen) at 33°C to maintain proliferation. Differentiation was induced by switching to 'non-permissive' condition transferring cells to 37°C and kept in culture for 7 days. The process of differentiation was evaluated using Western blotting and immunocytochemistry by determining the expression of the podocyte-specific marker podocin and the differentiation marker synaptopodin as shown in our previous work (Ambrus *et al.,* 2015). HEK293T cells were cultured in DMEM medium (PAA Laboratories GmbH) supplemented with 10% fetal bovine serum (Invitrogen), 50 $U{\cdot}mL^{-1}$ penicillin, 50 $\mu g{\cdot}mL^{-1}$ streptomycin, 1.25 $\mu g{\cdot}mL^{-1}$ Fungizone (both from PPA Laboratories GmbH) and non-essential aminoacids (Sigma-Aldrich, St Louis, MO, USA).

Antibodies

The following primary antibodies were employed for immunocytochemistry: mouse anti-human TRPV1, rabbit anti-human TRPV4 (both from Novus Biologicals, Littleton, CO, USA), rabbit anti-human **TRPV2** and rabbit anti-human **TRPV3** (both from Abcam, Cambridge, UK). For Western blotting, we used goat anti-human TRPV1 (Santa Cruz, Heidelberg, Germany), rabbit anti-human TRPV3, rabbit anti-human TRPV4 (Alomone Labs, Jerusalem, Israel), rabbit anti-human TRPV2 and rabbit-anti-human β-actin (ACTB) (Sigma-Aldrich).

Immunocytochemistry

Human podocytes were cultured and differentiated on glass coverslips in six-well plates, were fixed by 4% paraformaldehyde containing PBS (115 mM NaCl, 20 mM Na_2PO_4, pH 7.4; all from Sigma-Aldrich) for 10 min at room temperature and were permeabilized by 0.3% Triton-X-100 (Sigma-Aldrich) in PBS for 10 min. Following 30 min incubation in blocking solution (0.3% Triton-X-100 and 1% BSA containing PBS; both from Sigma-Aldrich) at room temperature, cells were probed with the previously mentioned primary antibodies raised against human TRPV1 (1:50), TRPV4 (1:50), TRPV2 (1:100) and TRPV3 (1:100) overnight at 4°C. Following appropriate washing in PBS, coverslips were incubated with Alexa-488®-conjugated goat-anti-mouse and goat-anti-rabbit secondary antibodies (1:200, Invitrogen) for 1 h at room temperature. Nuclei were counterstained with DAPI (Vector Laboratories, Peterborough, UK). Negative control cells were stained omitting the primary antibodies. Visualization of the proteins was performed by using Zeiss LSM 510 Meta Confocal Microscope (Zeiss, Oberkochen, Germany).

Western blot

Cells were harvested and homogenized in protease inhibitor cocktail (1:100; Sigma-Aldrich) containing detergent mixture (50 mM TRIS HCl, 150 mM NaCl, 1% Triton X-100, 1% Igepal CA 630, 0.5% sodium deoxicholate; Sigma-Aldrich). Protein

concentrations were determined by using BCA reagent (Pierce, Rockford, IL, USA) and set to 0.5 μg·mL^{-1}. Equal amount of protein samples (5 μg per well) were subjected to SDS-PAGE (10% Mini Protean TGX gels, BioRad, Hercules, CA, USA) and transferred to nitrocellulose membranes, by using Trans-Blot® Turbo™ Nitrocellulose Transfer Packs and Trans Blot Turbo System (both from BioRad). Membranes were probed with the corresponding primary antibodies overnight at 4°C. We applied anti-human TRPV1, TRPV2, TRPV4 (1:100) and TRPV3 (1:200) antibodies, diluted in 5% milk containing PBS. As secondary antibodies, horseradish peroxidase-conjugated rabbit anti-goat and goat anti-rabbit IgGs (1:1000, BioRad) were applied, and the immunoreactive bands were visualized by a SuperSignal West Pico Chemiluminescent Substrate-Enhanced Chemiluminescence kit (Pierce) using Gel Logic 1500 Imaging System (Kodak, Tokyo, Japan). To assess equal amount of protein in the different samples, we used β-actin as control, with rabbit anti-human β-actin antibody (1:1000, Sigma-Aldrich).

Transient overexpression of human recombinant TRPV channels

To check the specificity of the antibodies used in Western blot experiments, we transiently overexpressed human recombinant TRPV1–4 proteins in HEK293T cells and subjected the cell lysates to Western blotting. HEK293T cells cultured in 96 mm Petri dishes were transfected at 50–60% confluency using TransIT-293 Transfection Reagent (MirusBio, Madison, WI, USA). About 36 μL TransIT-293 reagent and 12 μL DNA construct were gently mixed in 600 μL OptiMEM (LifeTechnologies) medium, incubated for approximately 20 min and added to the cell cultures drop by drop. Following an incubation for additional 48 h, cells were harvested and analysed by Western blotting, as described above. As DNA constructs, sequence of human TRPV1 was cloned in the pCAGGSM2-IRES-GFP-R1R2 vector, and sequences of human TRPV2, TRPV3 and TRPV4 isoforms were cloned in the pCINeoIRES-GFP vector. The constructs were provided by Prof. Thomas Voets (Laboratory of Ion Channel Research, KU Leuven, Leuven, Belgium).

Gene silencing by RNA interference (RNAi)

Human podocytes were seeded in small Petri dishes or in 96-well black-wall/clear-bottom plates (Greiner Bio-One, Kremsmuenster, Austria) suitable for fluorescent measurements in culture medium. After podocytes differentiation, medium was changed to fresh culture medium and cells were transfected with siRNA oligonucleotides targeting human TRPV3 (Stealth RNAi, Invitrogen, ID: HSS136315) using Lipofectamine™ RNAiMAX Transfection Reagent and serum-free Optimem (both from Invitrogen). For controls, siRNA Negative Control Duplexes (scrambled RNA, Invitrogen) were employed. Forty-eight hours after transfection, cells in Petri dishes were harvested to quantitatively evaluate the efficacy of siRNA-driven silencing by Q-PCR and fluorescent Ca-measurements were performed on cells seeded in microplates.

Quantitative real-time PCR (Q-PCR)

To determine the quantitative expressions of various TRPs at the mRNA level, Q-PCR was performed on an ABI Prism 7000 sequence detection system (Applied Biosystems, Foster City, CA, USA) using the 5′ nuclease assay. Total RNA was isolated using TRIzol (Invitrogen) and reverse-transcribed into cDNA using High Capacity cDNA Reverse Transcription Kit (Applied Biosystems) and then amplified on a GeneAmp PCR System 2400 DNA Thermal Cycler (Applied Biosystems). PCR amplification was performed by using TaqMan primers and probes (assay ID-s: Hs00218912_m1 for TRPV1, Hs00275032_m1 for TRPV2, Hs00376854_m1 for TRPV3 and Hs00222101_m1 for TRPV4; all from Applied Biosystems). As internal controls, transcripts of peptidylprolyl isomerase A (PPIA; assay ID: Hs99999904_m1), GAPDH (assay ID: Hs99999905_m1) and β-actin (assay ID: Hs99999903_m1) were determined (all from Applied Biosystems). During the analysis, we used the geometric mean of the PPIA, GAPDH and β-actin as reference value.

Fluorescent Ca^{2+} measurements

Fluorescent measurement of cytoplasmic Ca^{2+} concentration was performed according to our previously optimized protocol: human podocytes were seeded in 96-well/clear-bottom plates (Greiner Bio-One) at a density of 20 000 cells per well in podocyte medium and cultured at 'non-permissive' conditions for 7 days. On the 7th day, the cells were washed once with Hanks solution ('normal buffer': 136.8 mM NaCl, 5.4 mM KCl, 0.34 mM Na_2HPO_4, 0.44 mM KH_2PO_4, 0.81 mM $MgSO_4$, 1.26 mM $CaCl_2$, 5.56 mM glucose, 4.17 mM $NaHCO_3$, pH 7.2, all from Sigma-Aldrich) containing 1% bovine serum albumin and 2.5 mM Probenecid (both from Sigma-Aldrich) then loaded with 1 μM Fluo-4 AM (Life Technologies Corporation, Carlsbad, CA, USA) dissolved in Hanks solution (100 μL per well) at 37°C for 30 min. The cells were washed three times with Ca^{2+}-containing (normal buffer) or Ca^{2+}-free (Ca^{2+}-free buffer) Hanks solution (100 μL per well). In the Ca^{2+}-free buffer, equimolar glucose substituted for $CaCl_2$. The plates were then placed into a FlexStation 3 fluorescent microplate reader (Molecular Devices, Sunnyvale, CA, USA), and cytoplasmic Ca^{2+} concentration (reflected by fluorescence; λ_{EX}: 494 nm, λ_{EM}: 516 nm) was monitored during application of compounds in various concentrations. During the measurements, cells in a given well were exposed to only one given concentration of the agents. When applying antagonists, cells were pretreated for 30 min and the measurements were carried out in the continuous presence of fixed concentration of the applied antagonist. Experiments were performed in multiple wells, and cells in different wells were cultured, differentiated and treated individually and independently. Data are presented as F_1/F_0, where F_0 is the average fluorescence of the baseline (before compound application) and F_1 is the actual fluorescence. During data analysis, *n* represents individual, independently measured wells.

To investigate the effect of a heat pulse on intracellular Ca^{2+} concentration, podocytes were seeded and differentiated in 35 mm diameter Petri dishes and loaded with 1 μM Fluo-4 AM (Life Technologies). Then, Petri dishes containing 300 μL ambient temperature normal buffer were placed on the stage of an Olympus IX83 inverted fluorescent microscope (Olympus, Tokyo, Japan), and Fluo-4 loaded cells were imaged with constant settings in every 9 s, using the autofocus mode between each capturing. During measurement, 1 mL pre-

heated solution was pipetted into the Petri dishes. Images were captured using an Xcellence Pro live cell imaging system (Olympus) and analysed in Fiji app running ImageJ software (Schindelin *et al.,* 2012, 2015).

Patch clamp recording

Podocytes were seeded in small Petri dishes and whole-cell patch clamp measurements were made by using an Axopatch 1.D amplifier and Clampex 10.2 software (Molecular Devices) on the next day. To record GSK-evoked transmembrane currents, experiments were performed in a bath solution containing 150 mM NaCl, 6 mM CsCl, 5 mM $CaCl_2$, 1 mM $MgCl_2$, 10 mM HEPES and 10 mM glucose buffered to pH 7.4 (NaOH), whereas the pipette solution consisted of 100 mM aspartic acid, 20 mM CsCl, 1 mM $MgCl_2$, 0.08 mM $CaCl_2$, 4 mM Na_2ATP, 10 mM EGTA, 10 mM HEPES and pH was set to 7.2 using CsOH resulted in approximately 100 mM Cs aspartate in the final pipette solution. The holding potential was 0 mV, and cells were ramped every 2 s from −120 to +100 mV over the course of 400 ms.

Curve fitting

Logistic dose–response curves were fitted using the equation y = A2 + (A1-A2)/(1 + (x/x0)^p) where the calculated parameters are as follows: A1: initial value (y_{min}); A2: final value (y_{max}); x0: centre (EC_{50}); and *P* is the calculated power. Fittings were carried out, and parameters were calculated using Origin 9.0 (OriginLab Corporation, Northampton, MA, USA).

Data and statistical analysis

The data and statistical analysis comply with the recommendations on experimental design and analysis in pharmacology (Curtis *et al.,* 2015). If not mentioned otherwise, data are presented as mean ± SEM. As the experiments were carried out on cell cultures using objective methods resulting in quantitative, interval scale numeric data which were analysed by properly chosen statistical methods, we discounted any influence of the experimenter's expectations on the results. Therefore, no randomization and blinding was performed. Normality of data was tested by Shapiro–Wilk test in each group. Means of multiple groups were compared by one-way ANOVA. If *F* achieved $P < 0.05$, pairwise comparison was done by appropriate *post hoc* tests. Homogeneity of variances was tested by Levene's test. If no inhomogeneity was found, ANOVA was followed by either Dunnett or Bonferroni *post hoc* tests, as appropriate. In case of inhomogeneous variances, Dunnett's T3 test was performed. To compare means of two groups with data not passing normality, Mann–Whitney *U*-test was performed. In every case, $P < 0.05$ was regarded as showing significant differences between group means. All statistical analysis was carried out using IBM SPSS Statistics 23.0 (IBM, Armonk, NY, USA).

Materials

Capsaicin, **capsazepine**, **eugenol**, **carvacrol**, **thymol**, 2-aminoethoxydiphenyl borate (**2-APB**), 4α-phorbol 12,13-didecanoate (**4α-PDD**) and **GSK1016790A** were obtained from Sigma-Aldrich. **AMG 9810**, **cannabidiol** (CBD) and **HC067047** were purchased from Tocris Bioscience (Bristol, UK) and **resiniferatoxin** from Santa Cruz (Santa Cruz, CA, USA). **Tranilast** was bought from Cayman Chemical Company (Ann Arbor, MI, USA). **Isopentenyl diphosphate** (IPP) was from Echelon Biosciences (Salt Lake City, UT, USA). **Ruthenium red** was obtained from Research Biochemicals International (Natick, MA, USA).

Nomenclature of targets and ligands

Key protein targets and ligands in this article are hyperlinked to corresponding entries in http://www.guidetopharmacology.org, the common portal for data from the IUPHAR/BPS Guide to PHARMACOLOGY (Southan *et al.,* 2016), and are permanently archived in the Concise Guide to PHARMACOLOGY 2015/16 (Alexander *et al.,* 2015a,b,c).

Results

First, we investigated the molecular expression of heat-sensitive TRPV1–4 channels in cultured, differentiated human podocytes. Immunocytochemical staining revealed a general expression of all the investigated proteins in differentiated human podocytes, although the staining for TRPV1 channels showed a relatively weaker signal compared to TRPV2–4 channels (Figure 1A). For Western blot, we have used selected antibodies of which specificity we have checked by probing human recombinant TRPV1–4 channels overexpressed in HEK-derived (HEK293T) cell line (Supporting Information Figure S1). The selected antibodies detected all the investigated TRPV isoforms both in differentiated and non-differentiated podocytes, although the molecular weight of the detected bands was not fully identical with the size of the bands detected in the recombinant cell line (Figure 1B). The podocytes-specific TRPV1 and TRPV2 bands were detected at a minimal higher molecular weight. The specific antibody detected multiple bands of the recombinant TRPV3 channels among which only one (approximately 60 kDa) was detected in podocytes. Interestingly, the TRPV4-specific antibody detected a very clear single band corresponding to the predicted molecular weight of the TRPV4 channel in HEK293T cells overexpressing the recombinant channel. However in podocytes, we could detect very intense signals but at definitely lower molecular weight. Nevertheless, each protein was detected both in differentiated and undifferentiated cells, as well. Generally, the intensity of all the TRPV1–4 immunoreactivity was found to be decreased in differentiated podocytes compared to undifferentiated cells. To further assess the quantitative expression of TRPV channels compared to each other, we studied the expression of specific TRPV transcripts by Q-PCR. We found that the expression of TRPV1 and TRPV4 was relatively high, but TRPV2 and TRPV3 protein were expressed at relatively low levels (Figure 1C).

As the molecular expression studies revealed a general expression of heat-sensitive TRPV channels, we investigated the functional responses for a thermal challenge applying a heat pulse by adding pre-warmed buffer to differentiated podocyte cultures. Because the studied channels are Ca^{2+}-permeable, their activity was investigated by monitoring the intracellular Ca^{2+} concentration using the fluorescent Ca^{2+}-sensitive reporter dye Fluo-4, upon heat stimulation. The majority of the cells reacted to the heat pulse with a transient elevation of the intracellular Ca^{2+} concentration (Figure 1 D–F, Supporting Information Videos S1 and S2), a response

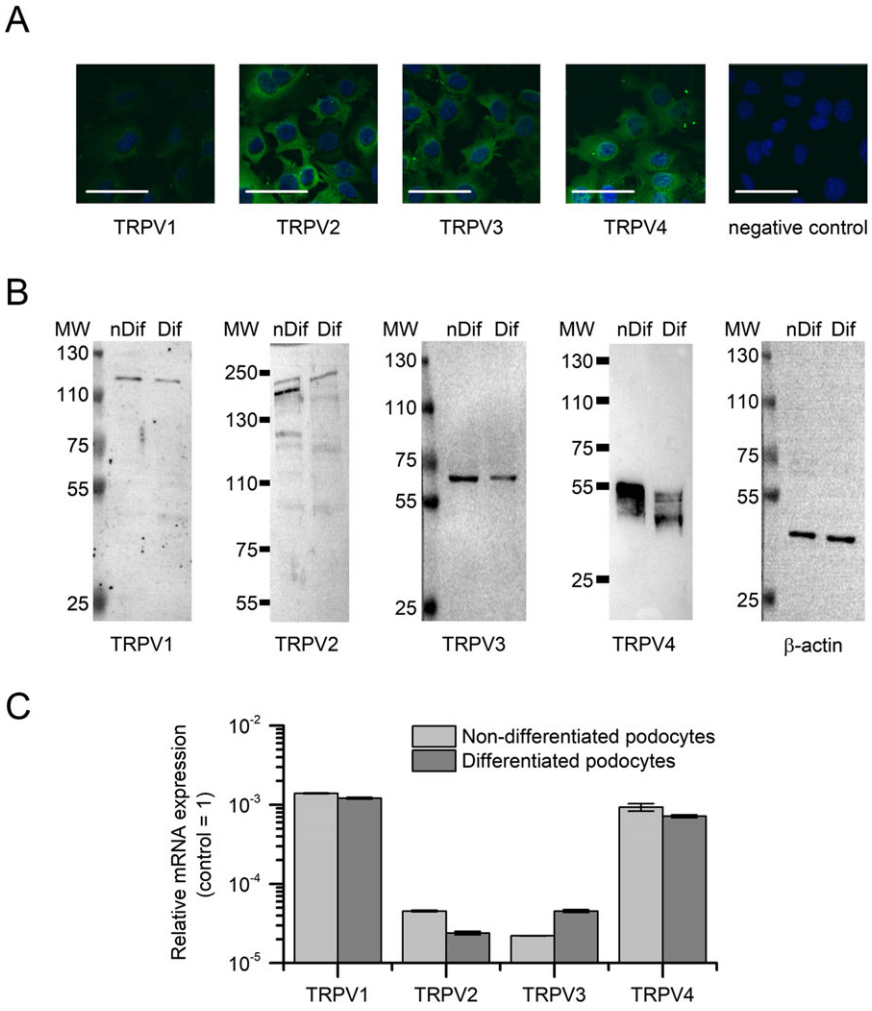

Figure 1

Expression of thermosensitive TRPV1–4 channels in differentiated human podocytes. (A) TRPV1–4 immunoreactivity was detected in differentiated human podocyte cultures by fluorescent labelling (Alexa-Fluor®-488, green fluorescence). Nuclei were counterstained with DAPI (blue fluorescence). Calibration mark: 50 μm. (B) Lysates of non-differentiated (nDif) and differentiated (Dif) human podocytes were subjected to Western blot analysis and immunolabelled with specific TRPV antibodies. To assess equal loading of protein samples, expression of β-actin was determined. MW indicates molecular weight in kDa. (C) Expression of TRPV1–4 mRNA transcripts was detected by Q-PCR in non-differentiated and differentiated human podocytes. Expression of PPIA (cyclophilin A), β-actin and GAPDH were determined, and the geometrical mean of their expression was used as internal control for normalization. Data are expressed as mean ± SEM, $n = 3$ independent determinations. (D) Representative images illustrating the effect of a heat pulse on differentiated podocytes. Cells were uploaded with the fluorescent Ca^{2+} sensitive dye Fluo-4 and challenged to a heat pulse. Arrowheads indicate representative cells displaying increase in intracellular Ca^{2+} concentration upon heat stimulation. (E) Representative Ca^{2+} traces obtained from the experiment shown in panel (D). The colours of the traces correspond to the colours of the arrowheads in panel (D). (F) Changes in intracellular Ca^{2+} concentration in differentiated podocytes upon control and heat pulse stimulations. Markings of the box plot represents 25 to 50 to 75 percentile of the cells, and thick line and whiskers indicate the mean and ±1 SD of the maximal Ca^{2+} signals respectively. *$P < 0.05$, significantly different as indicated; Mann–Whitney *U*-test.

which was not seen after applying ambient temperature as a stimulus (Figure 1F and Supporting Information Video S3). These results clearly indicated the presence of heat-sensitive Ca^{2+} channels in differentiated human podocytes. However, the applied heat pulse protocol was not specific enough to identify the individual heat-sensitive channels and discriminate between the contributions of the different TRPV isoforms which can exhibit partly overlapping temperature sensitivity in various conditions. Therefore, to judge the function of the individual TRPV isoforms, we used various pharmacological tools to activate these channels and assessed their specificity by applying specific antagonist pretreatments, if specific antagonists were available.

Capsaicin, a specific, potent activator of TRPV1 channels (Caterina *et al.*, 1997), did not induce any remarkable alteration in the intracellular Ca^{2+} concentration of the podocytes up to 1 mM. The presence of the TRPV1-specific antagonists, capsazepine or AMG 9810, did not influence the lack of the capsaicin effect (Figure 2A, B). Similarly, the ultrapotent TRPV1 channel agonist resiniferatoxin also failed to evoke

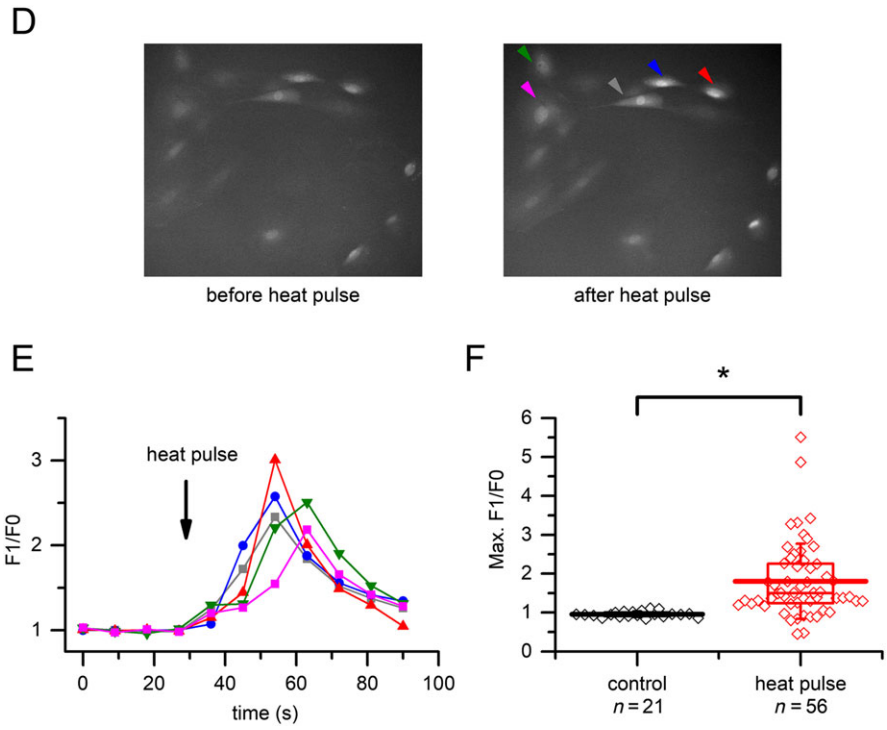

Figure 1
(Continued)

any response (Figure 2C). These results suggested that TRPV1, in spite of the relatively high expression of the mRNA transcripts, does not form a functional channel in the cultures of differentiated human podocytes.

The phytocannabinoid CBD, an agonist of both TRPV2 (Qin *et al.,* 2008) and TRPV4 channels (De Petrocellis *et al.,* 2012), induced a moderate elevation of intracellular Ca^{2+} concentration when applied at ≥10 μM concentration (EC_{50} = 10.6 ± 1.3 μM – Figure 3.). This effect was mainly eliminated by omitting the Ca^{2+} from the extracellular solution suggesting that CBD activated Ca^{2+}-permeable ion channels in the plasma membrane. The presence of 75 μM tranilast (Nie *et al.,* 1997), a potent ion channel inhibitor recently used to target TRPV2 channels (Hisanaga *et al.,* 2009; Mihara *et al.,* 2010; Perálvarez-Marín *et al.,* 2013), effectively inhibited the CBD-induced Ca^{2+} signals suggesting the presence of functionally active TRPV2 channels. However, CBD was also reported as a weak agonist of TRPV4 channels (De Petrocellis *et al.,* 2012). Therefore, we investigated the involvement of TRPV4 in the CBD-induced Ca^{2+} signals, repeating the experiments in the presence of HC067047, a potent and selective blocker of TRPV4 channels (Everaerts *et al.,* 2010). About 1 μM HC067047 inhibited the CBD-induced Ca^{2+} responses approximately as effectively, as tranilast did (Figure 3.), further confirming our previous results that CBD can activate TRPV4 channels (Oláh *et al.,* 2014) and suggesting the presence of functional TRPV4 channels in human podocytes.

To further dissect the functionality of TRPV4 channels, we investigated the effect of the hyper-potent TRPV4 channel agonist, GSK1016790A (Thorneloe *et al.,* 2008) on the intracellular Ca^{2+} concentration of podocytes. We found that GSK1016790A, applied at nM concentrations, induced a rapid and robust elevation of intracellular Ca^{2+} concentration which was strongly inhibited by the selective blocker of TRPV4 channels, HC067047 (EC_{50} values were 3.63 ± 0.33 and 57.07 ± 6.02 nM in the absence and presence of 1 μM HC067047 respectively; Figure 4A, B). Not only the peak but also the slope of the Ca^{2+}-transients was increased dose-dependently by GSK1016790A in Ca^{2+} containing buffer, even after the saturation of the Ca^{2+} signals, clearly indicating higher open probability of TRPV4 channels located in the plasma membrane (Figure 4C, D). GSK1016790A elevated the intracellular Ca^{2+} even in the absence of extracellular Ca^{2+}, although it was less potent (EC_{50} = 10.04 ± 0.72 nM) and definitely slower than in normal, Ca^{2+} buffer (Figure 4A–D), suggesting that functional TRPV4 channels are expressed on the intracellular Ca^{2+} stores, as well. However the much steeper rising phase in the presence of extracellular Ca^{2+} suggested that the majority of the channels are activated by the agonist in the plasma membrane (Figure 4D). The classical TRPV4 channel agonist 4α-PDD (Watanabe *et al.,* 2002) also raised the intracellular Ca^{2+} concentration (EC_{50} = 0.52 ± 0.06 μM), and its effect was also inhibited by HC067047, although 4α-PDD was less effective than GSK1016790A (Figure 4E, F). 4α-PDD-evoked responses were abolished in the absence of extracellular Ca^{2+} suggesting again that the majority of the activated TRPV4 channels are located in the plasma membrane. This was also supported by whole-cell patch clamp experiments in which we have detected strong GSK1016790A-induced

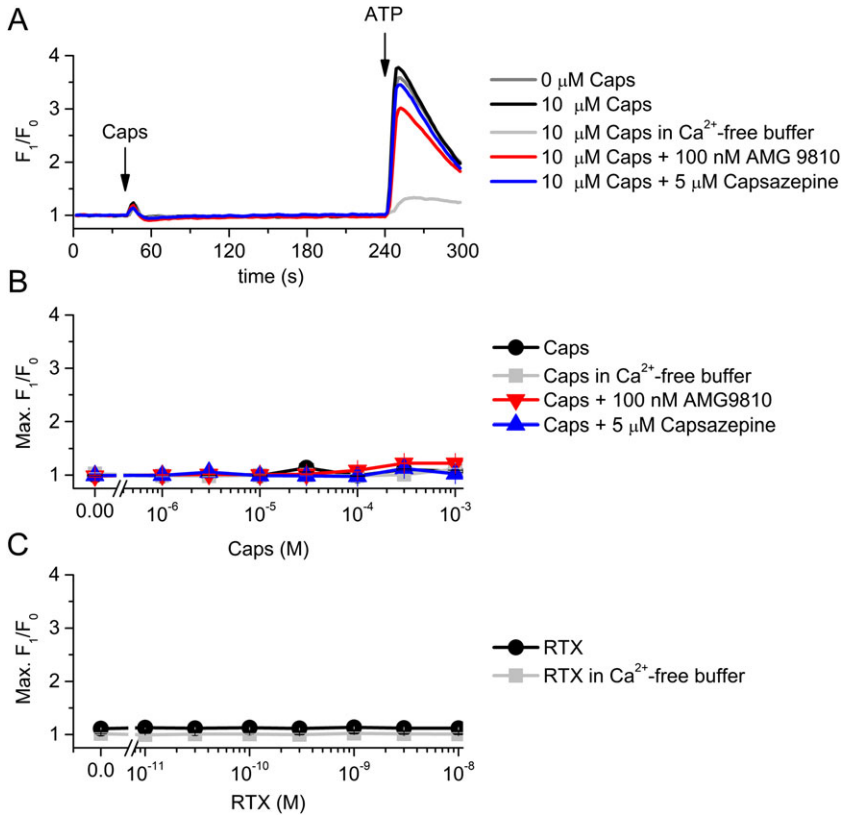

Figure 2

Effect of TRPV1 channel ligands on the intracellular Ca^{2+} concentration of differentiated human podocytes. (A) Representative time course of capsaicin (Caps) application in various conditions. Cells were preincubated with capsazepine and AMG 9810 for 30 min, and constant concentrations of the antagonists were presented as indicated on the figure continuously during the measurements. (B) Dose–response relationship of capsaicin in various conditions as indicated. The measurements were carried out as in panel (A). Data are means ± SEM, $n = 6$ in each group. (C) Dose-–response relationship of resiniferatoxin (RTX) in normal and Ca^{2+}-free buffer. The measurements were carried out as in panel (A), but RTX was applied instead of capsaicin. Data are presented as mean ± SEM, $n = 5$ in each group.

transmembrane currents whose biophysical characteristics corresponded to TRPV4 currents. Similarly to the Ca^{2+} signals, GSK1016790A-induced transmembrane currents were also inhibited by HC067047 (Figure 4G, H).

As specific agonist and antagonists are not available commercially, the pharmacological identification and separation of TRPV3 channels is the most challenging among heat-sensitive TRPV channels. Although they lack specificity, several herbal compounds, like eugenol, thymol or carvacrol, are reported as potent activators of TRPV3 channels (Xu *et al.,* 2006; Vriens *et al.,* 2008). Testing these compounds on differentiated human podocytes, we found a marked activation in the concentration range reported for effective activation of TRPV3 channels (Xu *et al.,* 2006; Vriens *et al.,* 2008), suggesting the presence of functional TRPV3 on human podocytes (Figure 5A, B.). However, the dose–response relationships were not saturated up to 1.5 mM and did not show sigmoid shape, suggesting that these compounds can activate other targets on podocytes, as well. In contrast, application of 2-APB, a synthetic but also not specific activator of TRPV3 channels (Chung *et al.,* 2004; Vriens *et al.,* 2009), significantly elevated cytoplasmic Ca^{2+} concentration from extracellular source resulting in a sigmoidal dose–response relationship (EC_{50} = 499 ± 51.2 μM) (Figure 5 C, D). Although the above compounds are effective activators of TRPV3 channels, all of them lack specificity and can affect cytoplasmic Ca^{2+} concentration *via* several other targets including other TRP channels, store operated Ca^{2+} entry or inositol trisphosphate **(IP_3) receptors**. Selected concentrations of carvacrol, thymol and 2-APB were only partially inhibited by the general, non-specific TRP channel inhibitor ruthenium red (≤35% inhibition); likewise, the endogenous TRPV3 inhibitor IPP (Bang *et al.,* 2011) partly inhibited only the 2-APB induced Ca^{2+} transients (~23% inhibition) (Figure 5E). Transfection of the podocytes with siRNA targeting TRPV3 channels resulted in a marked decrease in the expression of the channel compared to the scrambled RNA transfected control cells (Figure 5F). Although the TRPV3 silencing was found effective, it did not influence the Ca^{2+} responses evoked by the agonists shown above. These results indicate that although TRPV3 channel activators were effective in increasing cytoplasmic Ca^{2+} concentration of differentiated human podocytes, their application is likely to evoke several off-target effects and the contribution of TRPV3 channels to these Ca^{2+} responses is minimal.

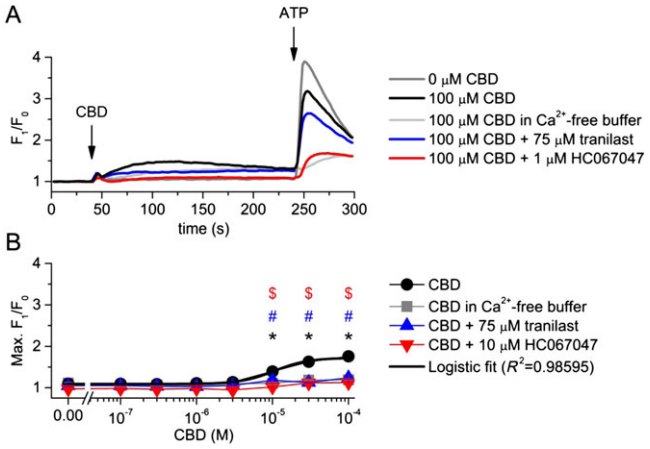

Figure 3

Effect of CBD on the intracellular Ca^{2+} concentration of differentiated human podocytes. (A) Representative time course of CBD applications in various conditions. Cells were preincubated with tranilast and HC067047 for 30 min, and measurements were carried out in the continuous presence of constant antagonist concentrations as indicated on the figure. (B) Dose–response relationship of CBD in various conditions as indicated. The measurements were carried out as in panel (A). Data are means ± SEM, $n = 6$ in each group. Logistic dose–response curve fitting was carried out as described in the 'Methods'. $^{*}P < 0.05$, significant difference between CBD and vehicle (0 μM CBD). $^{\#}P < 0.05$, significant inhibition by 75 μM tranilast. $^{\$}P < 0.05$, significant inhibition by 1 μM HC067047.

Discussion

In our current study, we provided the first evidence for the functional expression of the heat-sensitive members of the vanilloid subfamily of TRP channels in human podocytes. We described heat-evoked Ca^{2+} signals and detected the presence of TRPV1, 2, 3 and 4 proteins in the conditionally immortalized human podocyte cell line we have investigated. However, native TRPV3 and TRPV4 channels were detected at lower molecular weight in podocytes compared to the recombinant channels, which might suggest different degradation of these channels in the two cell lines. Quantitative analysis of the mRNA transcripts revealed that TRPV1 and TRPV4 are the dominantly expressed TRPV channels, but TRPV2 and TRPV3 channels were also detected at lower levels. These findings are highly consistent with publicly available microarray data of Da Sacco *et al.* (2013) (GEO Series accession number: GSE49439). Moreover, an additional transcriptome analysis (Boerries *et al.,* 2013) also detected TRPV1–4 transcripts in primary isolated mouse podocytes.

Dissecting the function of TRPV channels, we surprisingly found that the TRPV1-specific agonist capsaicin and the ultrapotent agonist resiniferatoxin failed to induce significant Ca^{2+} entry to podocytes suggesting loss of vanilloid sensitivity or an impaired function of TRPV1 channels in the investigated cell line. TRPV1 channels, earlier identified as the capsaicin receptors, are robustly activated by capsaicin in human and rodents. However, TRPV1 channels have been found to be insensitive to capsaicin in several other species (Jordt and Julius, 2002; Gavva *et al.,* 2004). Recent research revealed the molecular mechanism of capsaicin binding to TRPV1 channels and identified key amino acid residues, mutations of which decreased capsaicin sensitivity (Yang *et al.,* 2015). Single nucleotide polymorphisms in the human TRPV1 protein are also known to be associated with lowered capsaicin sensitivity (Cantero-Recasens *et al.,* 2010). Moreover, a capsaicin-insensitive splice variant TRPV1b has been identified, and its expression demonstrated in trigeminal and dorsal root ganglia (Lu *et al.,* 2005; Charrua *et al.,* 2008; Mistry *et al.,* 2014) and in keratinocytes (Pecze *et al.,* 2008). If TRPV1b is co-expressed with TRPV1, it behaves as dominant negative subunit disrupting capsaicin/vanilloid sensitivity of the channel (Vos *et al.,* 2006). In our case, both mutations in the key residues or the presence of the dominant negative subunit TRPV1b can be a rational explanation for the finding that in spite of the molecular expression of TRPV1 protein, we did not find any functional effect of capsaicin. Although desensitization by signalling pathways or functional inhibition by interacting partners, for example, phosphoinositols (Planells-Cases *et al.,* 2011; Rohacs, 2015), may also decrease the capsaicin sensitivity of TRPV1 channels, further studies are needed to identify the contribution of the different potential mechanisms.

In contrast to TRPV1, TRPV2 protein was detected not only at molecular level, but the presence of functional TRPV2 channels in the membrane of cultured human podocytes is strongly supported by our results showing that the TRPV2 channel agonist CBD induced a calcium influx from the extracellular space which was inhibited by tranilast, a suggested antagonist of TRPV2 channels. However, the specific TRPV4 channel blocker HC067047 also effectively inhibited CBD-induced Ca^{2+} entry. Therefore, we concluded that functional TRPV4 channels can also be involved in the effect of CBD. Indeed, the classical TRPV4 agonist 4α-PDD and the ultrapotent agonist GSK1016790A induced a rapid and robust increase in cytoplasmic Ca^{2+} concentrations which was strongly inhibited in the presence of the antagonist HC067047. In podocytes, GSK1016790A also induced marked transmembrane currents with a voltage-dependence characteristic for TRPV4 channels (Jin *et al.,* 2011) and blocked by HC067047. These functional results suggest that, in good accordance with the molecular expression data, TRPV4 channels are the dominantly expressed thermosensitive TRPV channels in human podocytes.

In contrast to TRPV4, the functional presence of TRPV3 channels was less clearly demonstrable. Although we identified the presence of TRPV3 proteins, quantitative analysis of expression of TRPV3 transcripts suggested a relatively low expression level compared to TRPV4. The pharmacological identification is uncertain since we lack commercially available, effective and highly specific TRPV3 channel agonists and antagonists. The botanical compounds carvacrol, thymol and eugenol, as well as the synthetic 2-APB used in our experiments, are potent but highly non-specific agonists, generally used to study TRPV3 channel functions (Chung *et al.,* 2004; Xu *et al.,* 2006; Vriens *et al.,* 2008, 2009). In human podocytes, all these compounds evoked marked elevation of the cytoplasmic Ca^{2+} concentration, mainly derived from the extracellular space (at least if compounds were applied at concentrations ≤1 mM), but only the effect of 2-APB reached a maximum over the concentration range

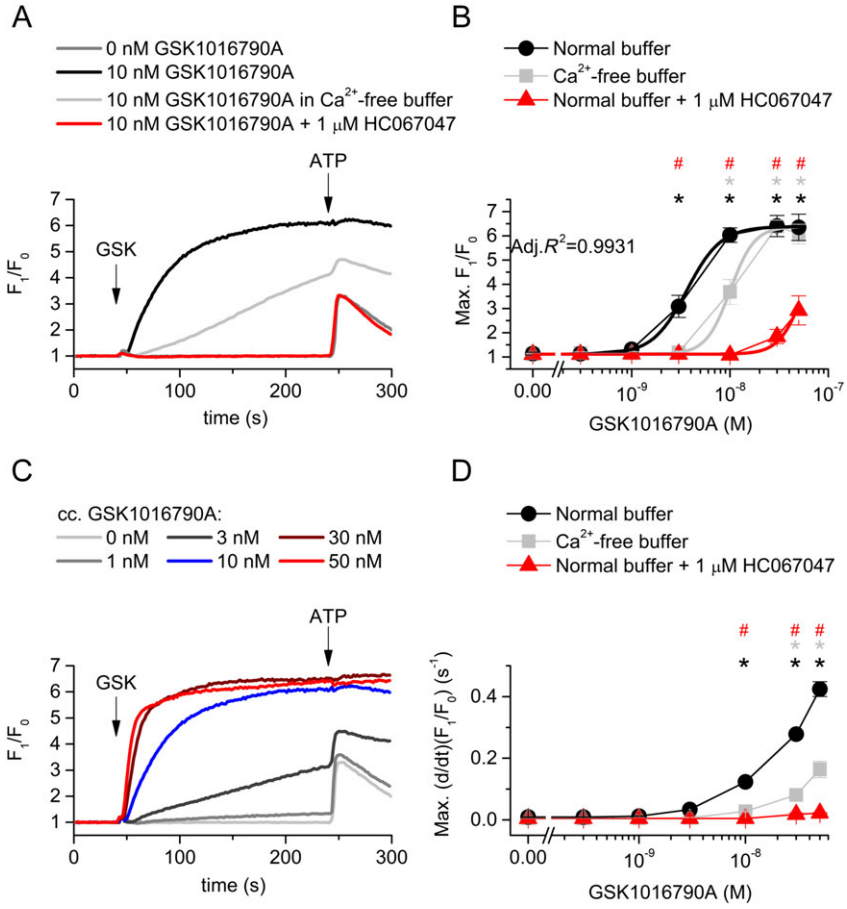

Figure 4

Activation of TRPV4 channels in differentiated human podocytes. (A) Representative time courses of the effect of the TRPV4 channel agonist GSK1016790A, in different conditions. Cells were preincubated with HC067047 for 30 min, and measurements were carried out in the continuous presence of constant antagonist concentrations as indicated on the figure. (B) Dose–response relationship of GSK1016790A in various conditions as indicated in the Figure. Measurements were carried out as shown in panel (A). Data are means ± SEM, $n = 6$ in each group. Logistic dose–response curve was fitted assuming equal efficacy (i.e. equal maximal responses available) in each condition. (C) Representative time courses upon application of various concentration of GSK1016790A in normal buffer illustrating the concentration dependence of the slope of the Ca^{2+} transients. (D) Concentration dependence of the maximal slope of the Ca^{2+} transients upon GSK1016790A application, $n = 6$ in each group. (E) Dose–response relationship of 4-αPDD in various conditions as indicated in the legend. Measurements were carried out as shown in panel (A), but 4-αPDD was used instead of GSK1016790A. Data are means ± SEM, $n = 5$ in each group. Logistic dose–response curve was fitted. (F) Concentration dependence of the maximal slope of the Ca^{2+} signals upon 4-αPDD application, $n = 5$ in each group. (G) Representative time courses illustrating the effect of GSK1016790A and HC067047 on transmembrane currents of podocytes measured at −80 and +80 mV. A voltage ramp from −120 to +100 mV was applied at every 2 s. (F) I–V relationship of the transmembrane currents at different time points as indicated in panel (E). In (B), (D), (E) and (F), $^{*}P < 0.05$, significant activation by GSK1016790A, compared with vehicle (0 nM GSK1016790A) control in the same conditions. $^{\#}P < 0.05$, significant inhibition by 1 μM HC067047.

applied, making possible the correct fitting of a sigmoidal dose–response curve. The experimentally determined EC_{50} (~500 μM) was higher than found earlier in electrophysiological studies on recombinant TRPV3 channels (~42 μM at physiological membrane potential; Chung *et al.*, 2004). Moreover, the non-selective TRP channel blocker, ruthenium red (Alexander *et al.*, 2015a), could only partly block the effect of the compounds, and the endogenous TRPV3 inhibitor IPP partly blocked only 2-APB evoked Ca^{2+} signals. In contrast, RNAi-mediated silencing of the molecular expression of TRPV3 protein did not alter the effects of the agonists. All these results argue for off-target effects of the TRPV3 channel ligands which can include the activation of several other TRP channels, and numerous other targets involved in cellular Ca^{2+} handling, such as the IP_3 receptors, **ryanodine receptors**, **sarcoplasmic reticulum Ca^{2+}-ATPase** or store operated Ca^{2+} entry mechanisms (Chung *et al.*, 2004; Xu *et al.*, 2006; Sárközi *et al.*, 2007; Vriens *et al.*, 2008, 2009; Hsu *et al.*, 2011; Liang and Lu, 2012). Therefore, although our results suggest that TRPV3 channels are expressed in human podocytes, their function is not clear. The exact role of this channels in the Ca^{2+} signals evoked by its activators needs further investigations. However, more specific pharmacological tools are needed to validate our results and further dissect the potential role of TRPV3 channels in podocytes.

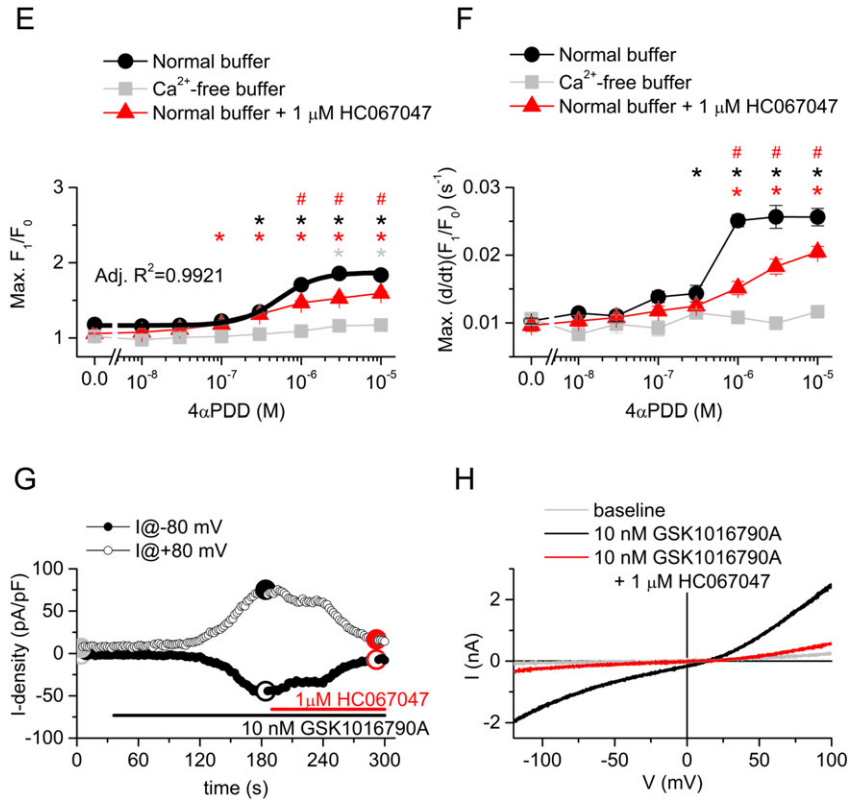

Figure 4
(Continued)

The expression of heat and mechanosensitive TRPV channels has been investigated in the lower urinary tract and in the kidney, ever since their cloning (Hayes *et al.*, 2000; Strotmann *et al.*, 2000; Kassmann *et al.*, 2013). Although there is clear evidence for the role of TRPV1 channels in the control of lower urinary tract functions, its expression in urothelial cells is still under debate (see, Franken *et al.*, 2014). The TRPV4 channel is more abundantly expressed in the non-neural cells of the urinary tract. In the kidney, TRPV4 expression was found overall in the constitutively water impermeable segments of the nephron (thin and thick ascending limb, distal convoluted tubule) and in the collecting ducts, as well (Tian *et al.*, 2004). Moreover, both TRPV1 and TRPV4 proteins were described to form functionally active channels in the endothelium of the renal vasculature (Chen *et al.*, 2015).

Although there is expression of heat-sensitive TRPV channels in the kidney, we lack a complete understanding of their functions in the different segments of the tubular epithelium, and we especially lack any data regarding podocytes. Although actually we do not have data about the physiological role of TRPV1–4 channels in regulating cellular functions of podocytes, it is well known that Ca^{2+} signalling related to other TRP channels, namely TRPC6 and TRPC5 channels, have a crucial impact on the biological functions of podocytes, influencing cytoskeletal rearrangements and consequently the physical characteristics of the slit diaphragm and the filtration barrier. Interestingly, TRPC5 and TRPC6 channels seem to oppositely regulate podocyte actin dynamics and cell motility *via* RhoA and Rac1 respectively (Tian *et al.*, 2010; Schaldecker *et al.*, 2013; Tian and Ishibe, 2016). Moreover, a recent study suggested that wild-type TRPC6 channels, but not the mutant allele TRPC6-N143S, originally described in a family with FSGS, showed intrinsic mechanosensitivity and responded to hypotonic challenges (Wilson and Dryer, 2014), suggesting a potential role of osmotic stimuli and consequent (TRP mediated) Ca^{2+} signals in the regulation of podocyte function.

In the renal tubular system, an important role in transmitting the effect of tubular flow and osmolarity is attributed to TRPV4 channels (Mamenko *et al.*, 2015). These channels mediated flow-induced increases in intracellular Ca^{2+} concentration in medullary thick ascending limbs (Cabral *et al.*, 2015), and their role was revealed in hypotonic stimuli-induced Ca^{2+} entry needed for regulatory volume decrease in renal cortical collecting duct cells (Galizia *et al.*, 2012). Beyond osmosensation, the TRPV4 channel seems to play an emerging role in the formation of epithelial barrier in several tissues. In airway epithelium, sheer stress enhanced epithelial barrier function *via* serial activation of TRPV4 channels and voltage-gated L-type Ca^{2+} channels (Sidhaye *et al.*, 2008). In epidermal keratinocytes of the skin, functionally active TRPV4 channels were found to interact

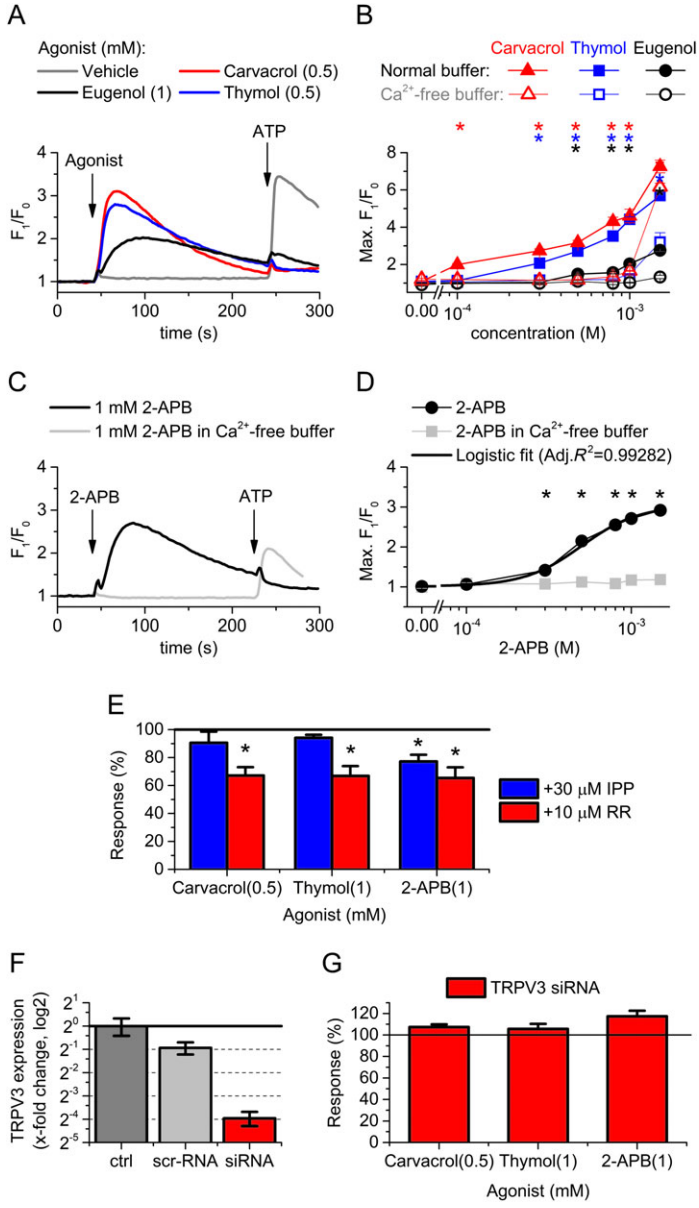

Figure 5

Effect of TRPV3 channel activators on the intracellular Ca^{2+} concentration of differentiated human podocytes. (A) Representative time courses showing the application of TRPV3 channel activators on differentiated human podocytes in normal buffer. Activators and ATP as positive control were applied as shown in the figure. (B) Dose–response relationship of carvacrol, thymol and eugenol in normal and Ca^{2+}-free buffer. Measurements were carried out as shown in panel (A). (C) Representative time courses showing the effect of 2-APB on differentiated human podocytes in normal and Ca^{2+}-free buffer. (D) Dose–response relationship of 2-APB treatment as shown in panel (C). (B and D) Data are means ± SEM, $n = 6$ in each group. *$P < 0.05$, significant activation by the compound indicated, compared with vehicle (0 μM compound) in normal buffer. (E) Effect of potential inhibitors of TRPV3 channels, ruthenium red (RR) and IPP on selected concentrations of carvacrol, thymol and 2-APB. Data are presented as percent of the average of the corresponding control (i.e. agonist application in the absence of the antagonist). This normalization was carried out to control the variance of the effectivity between different agonists and make comparable the inhibition evoked by the antagonists in the different groups. Response was calculated as the maximal amplitude (max. F_1/F_0–1) of the Ca^{2+} transients during the agonist application. Cells were pretreated with the inhibitors for 30 min before the agonist application, and the whole experiment was carried out in the continuous presence of the inhibitors in fixed concentration. Data are means ± SEM, $n = 6$ in each group. *$P < 0.05$, significant inhibition by IPP or ruthenium red; ANOVA with Dunnett *post hoc* test. (F) Changes in the expression of TRPV3 mRNA transcripts 48 h following transfection with either non-coding, scramled RNA (scr-RNA) or siRNA targeting TRPV3 (siRNA). Data are normalized to the average of the untransfected control to indicate the fold change in the expression of TRPV3 protein. Normalized data are presented as mean ± SEM of three independent determinations. (G) Effect of siRNA transfection targeting TRPV3 on the Ca^{2+} signals evoked by the indicated agonists. Measurements were carried out at 48 h after transfection. Averages of the corresponding control treatments on scrambled RNA transfected cells are considered as 100% in each case to control the variance of the effectivity between different agonists and make comparable the effect of the siRNA transfection in the different groups. Data are means ± SEM, $n = 6$ in each group.

with adherent junction proteins and actin cytoskeleton, enhancing cell–cell junction and tight barrier formation. In this process, TRPV4 channels contributed to the elevation of intracellular Ca^{2+} concentration resulting in small GTPase Rho activation and consequent actin rearrangement. Moreover, its pharmacological activation augmented tight junction development and barrier recovery (Sokabe *et al.,* 2010; Kida *et al.,* 2012; Akazawa *et al.,* 2013). Most recently, TRPV4 channels were described in bladder urothelium and kidney collecting duct epithelium associating with adherent junctions directly interacting with junctional proteins, especially α-catenin, an intracellular adherent junction protein connected to the actin cytoskeleton (Janssen *et al.,* 2016). All these data further suggest a putative contribution of TRPV4 channels to the fine orchestration of Ca^{2+} homeostasis in podocytes regulating the filtration barrier.

As podocytes in the outermost layer of the glomeruli form the final barrier to protein loss, their injury is often associated with marked proteinuria syndromes (Somlo and Mundel, 2000). Distinct diseases, like diabetic nephropathy, hypertension, as well as inherited or drug-induced podocytopathies, can result in disruption of the slit diaphragm leading to proteinuria (Mathieson, 2011). Although the detailed pathomechanism is still unknown, cytoskeletal disorganization as a consequence of the altered Ca^{2+} signalling can be an important step. Although the potential role of TRPV channels has not been investigated yet, numerous studies suggested the role of several elements of the cellular Ca^{2+} signalling pathways, such as those related to TRPC6 channels or angiotensin II receptors (Wieder and Greka, 2016). The activity of the TRPV channels, especially TRPV4, can be affected directly by the altered, disease-associated physical environment like increased flow and shear stress or altered osmotic concentrations, as detailed above. However, TRPV4 channels can be modulated by intracellular signalling pathways by, among others, angiotensin II signalling (Shukla *et al.,* 2010; Tajada *et al.,* 2017) which is of particular importance in podocytes (Hoffmann *et al.*, 2004). These potential integrative role of the TRPV(4) channels can make them especially appealing targets for future drug developments in various forms of podocyte-associated diseases.

All in all, although further studies are needed to clarify the potential role of TRPV channels in podocyte (patho) physiology, detailed understanding of their pharmacological role in physiological and disease conditions might contribute to the development of future therapies of primary and secondary podocytopathies and related kidney diseases.

Acknowledgements

The presented work was supported through the New National Excellence Program of the Ministry of Human Capacities and by Hungarian research grants OTKA 76065, NKFI K_16 120187, NKFI K_16 120552, TÁMOP-4.2.2.A-11/1/KONV-2012-0045 and LP003-2011/2015. B.I.T. is a recipient of the János Bolyai research scholarship of the Hungarian Academy of Sciences.

Author contributions

L.A., B.I.T. and B.K. designed and performed the experiments and collected and analysed the data. T.S.Z and T.B. designed and managed the research study. L.A., B.I.T. and T.B. wrote the paper which was carefully edited and reviewed by all other authors.

Conflict of interest

The authors declare no conflicts of interest.

Declaration of transparency and scientific rigour

This Declaration acknowledges that this paper adheres to the principles for transparent reporting and scientific rigour of preclinical research recommended by funding agencies, publishers and other organisations engaged with supporting research.

References

Akazawa Y, Yuki T, Yoshida H, Sugiyama Y, Inoue S (2013). Activation of TRPV4 strengthens the tight-junction barrier in human epidermal keratinocytes. Skin Pharmacol Physiol 26: 15–21.

Alexander SPH, Catterall WA, Kelly E, Marrion N, Peters JA, Benson HE *et al.* (2015a). The Concise Guide to PHARMACOLOGY 2015/16: Voltage-gated ion channels. Br J Pharmacol 172: 5904–5941.

Alexander SPH, Peters JA, Kelly E, Marrion N, Benson HE, Faccenda E *et al.* (2015b). The Concise Guide to PHARMACOLOGY 2015/16: Ligand-gated ion channels. Br J Pharmacol 172: 5870–5903.

Alexander SPH, Kelly E, Marrion N, Peters JA, Benson HE, Faccenda E *et al.* (2015c). The Concise Guide to PHARMACOLOGY 2015/16: Transporters. Br J Pharmacol 172: 6110–6202.

Alvarez DF, King JA, Weber D, Addison E, Liedtke W, Townsley MI (2006). Transient receptor potential vanilloid 4–mediated disruption of the alveolar septal barrier: a novel mechanism of acute lung injury. Circ Res 99: 988–995.

Ambrus L, Oláh A, Oláh T, Balla G, Saleem MA, Orosz P *et al.* (2015). Inhibition of TRPC6 by protein kinase C isoforms in cultured human podocytes. J Cell Mol Med 19: 2771–2779.

Bang S, Yoo S, Yang T-J, Cho H, Hwang SW (2011). Isopentenyl pyrophosphate is a novel antinociceptive substance that inhibits TRPV3 and TRPA1 ion channels. Pain 152: 1156–1164.

Boerries M, Grahammer F, Eiselein S, Buck M, Meyer C, Goedel M *et al.* (2013). Molecular fingerprinting of the podocyte reveals novel gene and protein regulatory networks. Kidney Int 83: 1052–1064.

Cabral PD, Capurro C, Garvin JL (2015). TRPV4 mediates flow-induced increases in intracellular Ca in medullary thick ascending limbs. Acta Physiol (Oxf) 214: 319–328.

Cantero-Recasens G, Gonzalez JR, Fandos C, Duran-Tauleria E, Smit LAM, Kauffmann F *et al.* (2010). Loss of function of transient receptor potential vanilloid 1 (TRPV1) genetic variant is associated with lower risk of active childhood asthma. J Biol Chem 285: 27532–27535.

Caterina MJ, Schumacher MA, Tominaga M, Rosen TA, Levine JD, Julius D (1997). The capsaicin receptor: a heat-activated ion channel in the pain pathway. Nature 389: 816–824.

Charrua A, Reguenga C, Paule CC, Nagy I, Cruz F, Avelino A (2008). Cystitis is associated with TRPV1b-downregulation in rat dorsal root ganglia. Neuroreport 19: 1469–1472.

Chen L, Kaßmann M, Sendeski M, Tsvetkov D, Marko L, Michalick L *et al.* (2015). Functional transient receptor potential vanilloid 1 and transient receptor potential vanilloid 4 channels along different segments of the renal vasculature. Acta Physiol (Oxf) 213: 481–491.

Chung M-K, Lee H, Mizuno A, Suzuki M, Caterina MJ (2004). 2-Aminoethoxydiphenyl borate activates and sensitizes the heat-gated ion channel TRPV3. J Neurosci 24: 5177–5182.

Curtis MJ, Bond RA, Spina D, Ahluwalia A, Alexander SPA, Giembycz MA *et al.* (2015). Experimental design and analysis and their reporting: new guidance for publication in BJP. Br J Pharmacol 172: 3461–3471.

Da Sacco S, Lemley KV, Sedrakyan S, Zanusso I, Petrosyan A, Peti-Peterdi J *et al.* (2013). A novel source of cultured podocytes. PLoS One 8: e81812.

De Petrocellis L, Orlando P, Moriello AS, Aviello G, Stott C, Izzo AA *et al.* (2012). Cannabinoid actions at TRPV channels: effects on TRPV3 and TRPV4 and their potential relevance to gastrointestinal inflammation. Acta Physiol (Oxf) 204: 255–266.

Dimke H, Hoenderop JGJ, Bindels RJM (2011). Molecular basis of epithelial Ca2+ and Mg2+ transport: insights from the TRP channel family. J Physiol 589: 1535–1542.

Dryer SE, Reiser J (2010). TRPC6 channels and their binding partners in podocytes: role in glomerular filtration and pathophysiology. Am J Physiol Renal Physiol 299: F689–F701.

Earley S, Brayden JE (2015). Transient receptor potential channels in the vasculature. Physiol Rev 95: 645–690.

Everaerts W, Zhen X, Ghosh D, Vriens J, Gevaert T, Gilbert JP *et al.* (2010). Inhibition of the cation channel TRPV4 improves bladder function in mice and rats with cyclophosphamide-induced cystitis. Proc Natl Acad Sci U S A 107: 19084–19089.

Feng N-H, Lee H-H, Shiang J-C, Ma M-C (2008). Transient receptor potential vanilloid type 1 channels act as mechanoreceptors and cause substance P release and sensory activation in rat kidneys. Am J Physiol Renal Physiol 294: F316–F325.

Franken J, Uvin P, De Ridder D, Voets T (2014). TRP channels in lower urinary tract dysfunction. Br J Pharmacol 171: 2537–2551.

Galizia L, Pizzoni A, Fernandez J, Rivarola V, Capurro C, Ford P (2012). Functional interaction between AQP2 and TRPV4 in renal cells. J Cell Biochem 113: 580–589.

Gavva NR, Klionsky L, Qu Y, Shi L, Tamir R, Edenson S *et al.* (2004). Molecular determinants of vanilloid sensitivity in TRPV1. J Biol Chem 279: 20283–20295.

Grace MS, Baxter M, Dubuis E, Birrell MA, Belvisi MG (2014). Transient receptor potential (TRP) channels in the airway: role in airway disease. Br J Pharmacol 171: 2593–2607.

Hayes P, Meadows HJ, Gunthorpe MJ, Harries MH, Duckworth DM, Cairns W *et al.* (2000). Cloning and functional expression of a human orthologue of rat vanilloid receptor-1. Pain 88: 205–215.

Hisanaga E, Nagasawa M, Ueki K, Kulkarni RN, Mori M, Kojima I (2009). Regulation of calcium-permeable TRPV2 channel by insulin in pancreatic beta-cells. Diabetes 58: 174–184.

Hoffmann S, Podlich D, Hähnel B, Kriz W, Gretz N (2004). Angiotensin II type 1 receptor overexpression in podocytes induces glomerulosclerosis in transgenic rats. J Am Soc Nephrol JASN 15: 1475–1487.

Hsu S-S, Lin K-L, Chou C-T, Chiang A-J, Liang W-Z, Chang H-T*et al.* (2011). Effect of thymol on Ca2+ homeostasis and viability in human glioblastoma cells. Eur J Pharmacol 670: 85–91.

Janssen DAW, Jansen CJF, Hafmans TG, Verhaegh GW, Hoenderop JG, Heesakkers JPFA *et al.* (2016). TRPV4 channels in the human urogenital tract play a role in cell junction formation and epithelial barrier. Acta Physiol (Oxf) 218: 38–48.

Jin M, Wu Z, Chen L, Jaimes J, Collins D, Walters ET*et al.* (2011). Determinants of TRPV4 activity following selective activation by small molecule agonist GSK1016790A. PloS One 6: e16713.

Jordt S-E, Julius D (2002). Molecular basis for species-specific sensitivity to 'hot' chili peppers. Cell 108: 421–430.

Kassmann M, Harteneck C, Zhu Z, Nürnberg B, Tepel M, Gollasch M (2013). Transient receptor potential vanilloid 1 (TRPV1), TRPV4, and the kidney. Acta Physiol (Oxf) 207: 546–564.

Kida N, Sokabe T, Kashio M, Haruna K, Mizuno Y, Suga Y*et al.* (2012). Importance of transient receptor potential vanilloid 4 (TRPV4) in epidermal barrier function in human skin keratinocytes. Pflüg Arch Eur J Physiol 463: 715–725.

Liang WZ, Lu CH (2012). Carvacrol-induced [Ca2+]i rise and apoptosis in human glioblastoma cells. Life Sci 90: 703–711.

Lu G, Henderson D, Liu L, Reinhart PH, Simon SA (2005). TRPV1b, a functional human vanilloid receptor splice variant. Mol Pharmacol 67: 1119–1127.

Mamenko M, Zaika O, Boukelmoune N, O'Neil RG, Pochynyuk O (2015). Deciphering physiological role of the mechanosensitive TRPV4 channel in the distal nephron. Am J Physiol Renal Physiol 308: F275–F286.

Mathieson PW (2011). The podocyte as a target for therapies – new and old. Nat Rev Nephrol 8: 52–56.

Mihara H, Boudaka A, Shibasaki K, Yamanaka A, Sugiyama T, Tominaga M (2010). Involvement of TRPV2 activation in intestinal movement through nitric oxide production in mice. J Neurosci 30: 16536–16544.

Mistry S, Paule CC, Varga A, Photiou A, Jenes A, Avelino A *et al.* (2014). Prolonged exposure to bradykinin and prostaglandin E2 increases TRPV1 mRNA but does not alter TRPV1 and TRPV1b protein expression in cultured rat primary sensory neurons. Neurosci Lett 564: 89–93.

Moran MM, McAlexander MA, Bíró T, Szallasi A (2011). Transient receptor potential channels as therapeutic targets. Nat Rev Drug Discov 10: 601–620.

Nie L, Oishi Y, Doi I, Shibata H, Kojima I (1997). Inhibition of proliferation of MCF-7 breast cancer cells by a blocker of Ca(2+)-permeable channel. Cell Calcium 22: 75–82.

Nilius B, Szallasi A (2014). Transient receptor potential channels as drug targets: from the science of basic research to the art of medicine. Pharmacol Rev 66: 676–814.

Oláh A, Tóth BI, Borbíró I, Sugawara K, Szöllősi AG, Czifra G *et al.* (2014). Cannabidiol exerts sebostatic and antiinflammatory effects on human sebocytes. J Clin Invest 124: 3713–3724.

Pecze L, Szabó K, Széll M, Jósvay K, Kaszás K, Kúsz E *et al*. (2008). Human keratinocytes are vanilloid resistant. PLoS One 3: e3419.

Perálvarez-Marín A, Doñate-Macian P, Gaudet R (2013). What do we know about the transient receptor potential vanilloid 2 (TRPV2) ion channel? FEBS J 280: 5471–5487.

Planells-Cases R, Valente P, Ferrer-Montiel A, Qin F, Szallasi A (2011). Complex regulation of TRPV1 and related thermo-TRPs: implications for therapeutic intervention. Adv Exp Med Biol 704: 491–515.

Qin N, Neeper MP, Liu Y, Hutchinson TL, Lubin ML, Flores CM (2008). TRPV2 is activated by cannabidiol and mediates CGRP release in cultured rat dorsal root ganglion neurons. J Neurosci 28: 6231–6238.

Retailleau K, Duprat F (2014). Polycystins and partners: proposed role in mechanosensitivity. J Physiol 592: 2453–2471.

Rohacs T (2015). Phosphoinositide regulation of TRPV1 revisited. Pflüg Arch Eur J Physiol 467: 1851–1869.

Saleem MA, O'Hare MJ, Reiser J, Coward RJ, Inward CD, Farren T*et al*. (2002). A conditionally immortalized human podocyte cell line demonstrating nephrin and podocin expression. J Am Soc Nephrol JASN 13: 630–638.

Sárközi S, Almássy J, Lukács B, Dobrosi N, Nagy G, Jóna I (2007). Effect of natural phenol derivatives on skeletal type sarcoplasmic reticulum Ca2+ -ATPase and ryanodine receptor. J Muscle Res Cell Motil 28: 167–174.

Schaldecker T, Kim S, Tarabanis C, Tian D, Hakroush S, Castonguay P *et al*. (2013). Inhibition of the TRPC5 ion channel protects the kidney filter. J Clin Invest 123: 5298–5309.

Schindelin J, Arganda-Carreras I, Frise E, Kaynig V, Longair M, Pietzsch T*et al*. (2012). Fiji: an open-source platform for biological-image analysis. Nat Methods 9: 676–682.

Schindelin J, Rueden CT, Hiner MC, Eliceiri KW (2015). The ImageJ ecosystem: an open platform for biomedical image analysis. Mol Reprod Dev 82: 518–529.

Shukla AK, Kim J, Ahn S, Xiao K, Shenoy SK, Liedtke W*et al*. (2010). Arresting a transient receptor potential (TRP) channel: beta-arrestin 1 mediates ubiquitination and functional down-regulation of TRPV4. J Biol Chem 285: 30115–30125.

Sidhaye VK, Schweitzer KS, Caterina MJ, Shimoda L, King LS (2008). Shear stress regulates aquaporin-5 and airway epithelial barrier function. Proc Natl Acad Sci U S A 105: 3345–3350.

Sokabe T, Fukumi-Tominaga T, Yonemura S, Mizuno A, Tominaga M (2010). The TRPV4 channel contributes to intercellular junction formation in keratinocytes. J Biol Chem 285: 18749–18758.

Somlo S, Mundel P (2000). Getting a foothold in nephrotic syndrome. Nat Genet 24: 333–335.

Southan C, Sharman JL, Benson HE, Faccenda E, Pawson AJ, Alexander SPH *et al*. (2016). The IUPHAR/BPS guide to PHARMACOLOGY in 2016: towards curated quantitative interactions between 1300 protein targets and 6000 ligands. Nucl Acids Res 44: D1054–D1068.

Strotmann R, Harteneck C, Nunnenmacher K, Schultz G, Plant TD (2000). OTRPC4, a nonselective cation channel that confers sensitivity to extracellular osmolarity. Nat Cell Biol 2: 695–702.

Tajada S, Moreno CM, O'Dwyer S, Woods S, Sato D, Navedo MF *et al*. (2017). Distance constraints on activation of TRPV4 channels by AKAP150-bound PKCα in arterial myocytes. J Gen Physiol 149: 639–659.

Thorneloe KS, Sulpizio AC, Lin Z, Figueroa DJ, Clouse AK, McCafferty GP *et al*. (2008). N-((1S)-1-{[4-((2S)-2-{[(2,4-dichlorophenyl)sulfonyl] amino}-3-hydroxypropanoyl)-1-piperazinyl]carbonyl}-3-methylbutyl)-1-benzothiophene-2-carboxamide (GSK1016790A), a novel and potent transient receptor potential vanilloid 4 channel agonist induces urinary bladder contraction and hyperactivity: Part I. J Pharmacol Exp Ther 326: 432–442.

Tian D, Jacobo SMP, Billing D, Rozkalne A, Gage SD, Anagnostou T *et al*. (2010). Antagonistic regulation of actin dynamics and cell motility by TRPC5 and TRPC6 channels. Sci Signal 3: ra77.

Tian W, Salanova M, Xu H, Lindsley JN, Oyama TT, Anderson S *et al*. (2004). Renal expression of osmotically responsive cation channel TRPV4 is restricted to water-impermeant nephron segments. Am J Physiol Renal Physiol 287: F17–F24.

Tian X, Ishibe S (2016). Targeting the podocyte cytoskeleton: from pathogenesis to therapy in proteinuric kidney disease. Nephrol Dial Transplant 31: 1577–1583.

Tóth BI, Nilius B (2015). Chapter 2 – transient receptor potential dysfunctions in hereditary diseases: TRP channelopathies and beyond A2 – Szallasi, Arpad. In: TRP Channels as Therapeutic Targets. Academic Press: Boston, pp. 13–33.

Tóth BI, Oláh A, Szöllősi AG, Bíró T (2014). TRP channels in the skin. Br J Pharmacol 171: 2568–2581.

Vos MH, Neelands TR, McDonald HA, Choi W, Kroeger PE, Puttfarcken PS *et al*. (2006). TRPV1b overexpression negatively regulates TRPV1 responsiveness to capsaicin, heat and low pH in HEK293 cells. J Neurochem 99: 1088–1102.

Vriens J, Appendino G, Nilius B (2009). Pharmacology of vanilloid transient receptor potential cation channels. Mol Pharmacol 75: 1262–1279.

Vriens J, Nilius B, Vennekens R (2008). Herbal compounds and toxins modulating TRP channels. Curr Neuropharmacol 6: 79–96.

Watanabe H, Davis JB, Smart D, Jerman JC, Smith GD, Hayes P *et al*. (2002). Activation of TRPV4 channels (hVRL-2/mTRP12) by phorbol derivatives. J Biol Chem 277: 13569–13577.

Wieder N, Greka A (2016). Calcium, TRPC channels, and regulation of the actin cytoskeleton in podocytes: towards a future of targeted therapies. Pediatr Nephrol Berl Ger 31: 1047–1054.

Wilson C, Dryer SE (2014). A mutation in TRPC6 channels abolishes their activation by hypoosmotic stretch but does not affect activation by diacylglycerol or G protein signaling cascades. Am J Physiol Renal Physiol 306: F1018–F1025.

Woudenberg-Vrenken TE, Bindels RJM, Hoenderop JGJ (2009). The role of transient receptor potential channels in kidney disease. Nat Rev Nephrol 5: 441–449.

Xu H, Delling M, Jun JC, Clapham DE (2006). Oregano, thyme and clove-derived flavors and skin sensitizers activate specific TRP channels. Nat Neurosci 9: 628–635.

Yang D, Luo Z, Ma S, Wong WT, Ma L, Zhong J *et al*. (2010). Activation of TRPV1 by dietary capsaicin improves endothelium-dependent vasorelaxation and prevents hypertension. Cell Metab 12: 130–141.

Yang F, Xiao X, Cheng W, Yang W, Yu P, Song Z *et al*. (2015). Structural mechanism underlying capsaicin binding and activation of the TRPV1 ion channel. Nat Chem Biol 11: 518–524.

Supporting Information

Additional Supporting Information may be found online in the supporting information tab for this article.

https://doi.org/10.1111/bph.14052

Figure S1 Specificity of the antibodies used to detect TRPV1–4 in western blot. Control HEK293T cells (HEK) and HEK293T cells overexpressing human recombinant TRPV1–4 isoforms (+hrV1–4) following a transient transfection with the corresponding DNA constructs were subjected to western blot and probed with anti-TRPV1, anti-TRPV2, anti-TRPV3 and anti-TRPV4 antibodies as described in the 'Methods' section. The antibodies demonstrated high specificity, they detected only the targeted isoform and showed no unspecific staining in the human embryonic kidney originated cell line.

Video S1 Supplementary video files demonstrate time laps videos converted from representative Ca2+ imaging experiments applying heat pulse (Supplementary video file 1–2) or ambient temperature as control (Supplementary video file 3) stimulations on human differentiated podocytes. Cells were previously loaded with Fluo-4 AM calcium indicator and stimulated as described in the 'Methods' section.